Institute of Theoretical
and Experimental Physics

26-99

A.L. Suvorov, V.F. Elesin, K.N. Eltsov, M.A. Kozodaev,
A.V. Krasheninnikov, O.N. Makeev, L.A. Openov,
M.O. Popov, Yu.N. Cheblukov, V.Yu. Yurov

QUANTITATIVE SCANNING TUNNELING MICROSCOPY OF RADIATION EFFECTS ON SURFACES OF SOLIDS

Moscow 1999

UDK 537.534.35 M-16

QUANTITATIVE SCANNING TUNNELING MICROSCOPY OF RADIATION EFFECTS ON SURFACES OF SOLIDS: Preprint ITEP 26-99/

A.L. Suvorov, V.F. Elesin, K.N. Eltsov, M.A. Kozodaev, A.V. Krasheninnikov, O.N. Makeev, L.A. Openov, M.O. Popov, Yu.N. Cheblukov, V.Yu. Yurov-
M., 1999 - 24p.

The advanced areas of scanning tunneling microscopy application in the investigation of radiation effects on surfaces and in sub-surface layers of solids are reviewed and analyzed. A classification of works is proposed: by the types of irradiation exposures, by the energies of bombarding particles and irradiation fluences, by the investigated materials and effects. Definitions are given of the problems of radiation damage physics of solids, which may be solved to advantage with the help of scanning tunneling and atomic-force microscopy. The problems cover, in the first place, the sub-threshold effects of sputtering and atoms displacement; quantitative estimation of crystalline lattice deformation in the regions of various-type defects; single events of bombarding particles interaction with the surfaces of materials; cascade effects in the subsurface regions of materials; quantitative estimates (also employing the notion of fractal dimensions) of the surface geometry evolution with regard to the nature of the bombarding particles, their energies, and irradiation parameters. The paper underscores the importance of the discussed technique application in radiation technologies refinement. Examples are given of the results of concrete investigations in the discussed field carried out by the authors.

Fig. - 12, ref. - 29 name.

I. INTRODUCTION

As a rule, materialization of practically any new experimental technique (especially so imposing a technique, both in principles and capabilities, as scanning tunneling microscopy, or STM [1]) is accompanied with an outburst of activity of scientists working in various fields. The result is the emergence of multiple publications reporting the first results of the new technique application in solving a wide range of problems. The tasks posed are often extremely exotic and not always well-defined in terms of logic. In such situation, many researchers, lead by a noble impulse, pioneer the new technique applications in various fields of science, in study of new phenomena, new objects, etc. With the lapse of time, however (which may be years or decades), the rush of the first moments subsides in certain areas – to make room for serious thought. The question is raised, and the answers are sought, whether the application of the now relatively new technique is justified in one or the other field, or line of research of one or the other class of objects. In many a case there comes an understanding that the new technique may be making absolutely no sense, being no match for other experimental methods, its use in a particular direction having no prospects. The less prospective directions are screened and discarded even within one narrow field, to concentrate the effort on other directions in the same field.

Such, in our opinion, is the situation in the field of scanning tunneling microscopy (in no less degree, of atomic-force microscopy, or AFM) [2] application in radiation damage physics of solids (RDPS) and radiation materials science (RMS). At present, over a hundred publications covering the subject in this way or other have come out of the press. It was in this field that the named outburst of activity had been registered. Now a new outlook is being formed on where, along which lines of research in the said field is scanning tunneling microscopy found to be beyond all competition, bringing really new, original and valuable information.

This paper presents an attempt to classify the presently completed works in the described field, to look into the most promising fields of research, as well as to give original examples in illustration to both.

II. PROPOSED CLASSIFICATION

The idea of the proposed classification is to examine the abundance of the currently available information, set clear the task of discriminating the most promising lines of research, and finally try to arrive at a grounded conclusion whether radiation damage physics of solids and radiation materials science are the areas where the experimental technique in question may open an opportunity to say something new. It should be noted, however, that the proposed classification is absolutely conditional and is subject to clarification and improvement.

II.1. Materials. Bearing in mind the specific character of scanning tunneling microscopy, which allows to examine successfully the surfaces with sufficiently large atom-smooth areas, and the surfaces of the classes of materials traditionally investigated in RDPS, let us rank different materials in the following sequence: carbon materials, among them, primarily: graphites, diamonds and diamond-like materials, nanocluster carbon structures [3] (M-1); semiconductors (M-2); metals and alloys (M-3); dielectrics (M-4). Note here that the majority of the currently known works analyzed high-oriented pyrolitic graphite (HOPG) and silicon, although beside them, the radiation effects were also investigated in a number of pure metals and a few other materials [4 – 6].

II.2. Types of irradiation. Here, with but a few reservations, use may be made of a more or less standard classification [7, 8]: light ions (P-1), heavy ions, including nuclear fission products (P-2); electrons (P-3); neutrons (P-4); γ-quanta, including laser (P-5); plasma (P-6); nanoparticles (P-7). It should be noted that, as of today, scanning tunneling microscopy has found application in investigating all of the named irradiation types, although the results are, in the major part, of purely qualitative – often demonstrative – kind.

II.3. Particle energies. Here we have reason again to resort to the standard classification of particles by their energies: sub-threshold, i.e., close-to-threshold energies of crystal lattice atomic displacements or surface atoms sputtering [7, 9] (E-1); low energies from several hundred eV to several keV in the region of transition to the cascade-forming (in case of ions) irradiation (E-2); medium energies of tens and hundreds keV (E-3); high energies of tens and hundreds MeV (E-4). It is clear that for electrons, γ-quanta and plasma, the numerical values of the energy intervals will be different, although in their case classification may also be conditionally used. A more logical, approach would be to reduce the number of energy intervals, but at present this is not imperative. By now, partly qualitative and partly quantitative results have been obtained for all energy intervals.

II.4. Irradiation fluences. Obviously, three intervals will suffice here: single hits of bombarding particles, when overlapping of the traces of their interaction with the surface is hardly registered (F-1), small fluences, when the traces of single hits overlap but infrequently, and both types of effects are registered in the field of vision of the microscope (F-2); high fluences, when the particle hits follow one after the other and overlap multiply (F-3).

II.5. Irradiation and annealing temperatures. The sample may have different temperatures in the course of irradiation and the subsequent microscopic analysis. Since investigation of the annealing processes presents a scientific and practical interest in RDPS and RMS, for the purposes of analysis and classification of the works in question, these two temperatures should be regarded separately: every time the temperatures are discussed, their origin should be noted. Logically, the "irradiation" temperatures may be subdivided into three ranges: cryogenic (IT-1), or temperatures at which the majority of processes (e.g., migration of interstitial atoms) is frozen; low (IT-2), or temperatures close to room temperature, at which the processes of crystal structure recovery still remain insignificant; and high temperatures (IT-3), corresponding to realization of all stages of annealing. For further investigation of defects annealing, additional classification of the experiment temperatures as per the annealing stages may be introduced, e.g. PIAT-3, or the temperature of stage 3 of post-irradiation annealing, etc.

II.6. Investigated effects. With all the variety of radiation effects, the main effects may also be arranged in a reasonable classification. It is clear that the selection of such effects will be determined by the purpose of the investigation being carried out. At the same time, the selection itself will govern the type of the classification parameters as per the preceding five clauses. We will limit ourselves to the effects which are normally investigated with scanning tunneling (and atomic-force) microscopy (the list may be extended if necessary): formation of single point defects and crystal lattice distortions due to them (D-1); single point defects mobility, their interaction, formation of low-ratio point defect complexes close to material surface (D-2); surface atoms sputtering, particularly the specific features of this process in the existing defects areas: grain boundaries, steps, etc. (D-3); formation of tracks presenting the defect areas at points of bombarding particles entry into the material volume (D-4); macroscopic (multi-atom) changes in surface relief and regular structures formation (D-5); appearance of incipient micro-cracks close to surface (D-6); initial stages of blistering and flaking [10] (D-7); subsurface defects annealing (D-8). At present, investigations in all of the above directions have been started.

III. SPECIFIC FEATURES OF EXPERIMENT

In this section, general comments are offered concerning the specific features of the conducted investigations.

III.1. Investigated materials. The choice of the STM investigation procedure is to a great extent defined by the type of the analyzed material. Obviously, scanning tunneling microscopy is able to yield better results in investigation of current-conducting materials. In principle, it may be applicable in dielectrics investigation as well, but in this case the replication method [11], widely spread in transmission electron microscopy, need be resorted to, with the one modification: the replica created, e.g., by magnetron deposition, need not be removed. It is then scanned directly on the sample surface. It is also clear that for work with the materials with oxidation-prone surface super-high vacuum devices should be used.

III.2. Used devices. The type of the devices used is determined both by the material taken for the analysis, and the purpose of the investigation. For study of surface reliefs of "non-oxidizing" materials (D-5, D-6, D-7), it is reasonable to use microscopes operating in the air. When atomic-scale resolution is required, and for analyzing atomic displacements in the region of point defects and their complexes, super-high vacuum devices are more preferable. Naturally, such a device must have a surface cleaning system, e.g., with the use of ion beams. In a number of cases, irrespective of the investigated material being conducting or non-conducting, it makes sense to resort to atomic-force microscopic analysis. The AFM and the STM results may then be compared and mutually corrected. It is extremely useful, as an addition, to combine microscopic analysis with other informative methods, such as, e.g., Auger-electron spectroscopy, etc. It is a requirement of today that the used devices provide an opportunity to conduct investigations at both cryogenic high temperatures.

III.3. Irradiation sources. Apparently, any types of irradiation sources may be used for the investigations discussed, provided the irradiated samples are handled in compliance with the radiation safety regulations. In case of vacuum microscopes and in conducting the investigations as per items D-1 and D-2 and a few others, it is extremely important to have the irradiation source installed directly within the vacuum volume of the device.

IV. EFFECTS OF MATERIALS IRRADIATION WITH PARTICLES OF CLOSE-TO-THRESHOLD ENERGIES

The review of the results obtained by other authors is found in paper [4]. In the majority of them HOPG is mentioned. It should be noted that HOPG investigation presents a practical interest (it finds wide application in reactor engineering, microelectronics and a few other fields), as well as a methodological interest. In fact, this material is chemically inert and allows work in the air, its quasi-two-dimensionality facilitates its spalling along planes, producing smooth, up to 100 nm long, sections along the spallation planes, which is most convenient for ions irradiation and further STM and

AFM analysis. And finally, graphite (and other graphite materials) is looked upon as a unique material from the point of view of fundamental physics. The flexibility of its valence bonds in equilibrium and non-equilibrium conditions under irradiation brings about a variety of phase transformations and structures. Meanwhile, interpretation and the theory of the transformation mechanisms are far from being complete. At the same time, new theoretical approaches have appeared in the last 10 – 15 years. They allow to estimate the real structure of molecules, clusters and solid bodies proceeding from the primary principles. So, it was proved in [12] that defects (e.g., interstitials) may get attracted to each other in graphite at the expense of lattice deformation.

The recently obtained results of STM analysis of the HOPG surface structure irradiated with single gas ions of sub-threshold energies testify to the deformation-type mechanism of interaction. Depending on its energy, the bombarding ion gets under the first atomic layer of graphite surface, creating, or not creating, a vacancy. It is worth notice that in all STM investigations carried out in the air the defects looked practically the same: as hillocks, despite that, with the energies exceeding the threshold energy of displacement, there is probability of generation of a variety of defects. Apparently, one of the first experiments under conditions of super-high vacuum (SHV) was the one carried out by a group of authors of the present paper [13]. Clearly, investigations under SHV allow to exclude the influence of such external factors as, e.g., adsorbate. In the latter experiment, HOPG samples were irradiated with Ar^+ ions with energies of 45 and 55 eV. Irradiation was carried out in the SHV-STM intermediate chamber [14]; the ion current was $2 \cdot 10^{-9}$ A, the irradiation time was several minutes. The resulting image in the 50 × 50 nm field of vision showed about 10 defects, which means that there was no overlapping of single ion hits. After irradiation, the sample was transferred to the STM chamber for investigation.

An example of various defects obtained in the first series of experiments of irradiation with 45-eV ions, as observed in an STM image, is given in Fig. 1. It may be seen clearly that the two defects in the top part show as

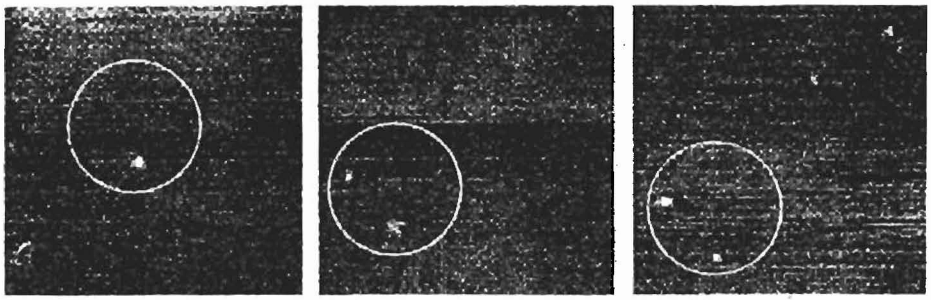

Fig. 1. *STM images of defects of HOPG surface after irradiation with 45-eV Ar^+ ions. The circle indicates one and the same are for pictures a, b and c. Scanning parameters: U_s = 0.7 V, I_t = 1.0 nA. All three pictures are of one size: 49 × 49 nm^2. For estimation: the "bright" defect height is about 0.5 nm, the depth of "dark" defects is about 0.4 nm.*

dark spots: they correspond to pits in the STM image. The defect in the bottom part seen as a bright spot corresponds to a hillock. The contrast between the dark and bright defects is particularly strong at voltage across the sample being U_s = –0.4 V. As voltage across the sample increased to –0.9 V, the dark defects changed to small bright spots inside a dark rim or semicircle. With voltage drop back to –0.4 V, the dark image of the defect recovers. Such variations in the image of the dark defects were observed many times in different HOPG samples, naturally, with different needles. With voltage variation across the sample, the bright defects underwent no serious changes. To all appearance, such a difference in the obtained images of defects is related to the differences in the distribution of densities of the electron states, which, in its turn, may testify to a different nature of the defects in question. The bright defects height was about 0.5 nm. The dark spots depth was about 0.4 nm.

Another interesting feature of the dark defects is connected with their ability to undergo irreversible changes in the process of scanning, which is confirmed in the series of STM images shown in Fig. 1. In the presented series, the sequence of several recorded pictures shows the left dark defect going bright, and the right dark defect disappear. At that, all initially bright defects remain practically unchanged. The authors failed to achieve atomic-scale resolution in the central part of the observed defects picture. The used tungsten needles (probes) ensured good atomic-scale resolution around the defects, but within the defect proper the structure of hillocks remained always disordered. A characteristic image of a bright defect is given in Fig. 2.

Fig. 2. *STM image of a single "bright" defect of HOPG surface after irradiation with 45-eV Ar^+ ions. The atomic structure of graphite is observed around the defect. Scanning parameters: $U_s = 0.05$ V, $I_t = 0.5$ nA. Picture size: 6.8 × 6.8 nm^2. "Hillock" height: about 0.3 nm.*

Image scanning parameters: $U_s = 0.05$ V; tunnel current $I_t = 0.5$ nA; picture size 6.8 × 6.8 nm^2; hillock height about 0.3 nm. The presented results are original and, beside all, allow to conclude that the dark defects present vacancies, and the bright defects present either interstitials, or vacancies with the already entrapped atomic clusters.

V. THEORETICAL COMPUTATION AND COMPUTER SIMULATION OF STM IMAGES

In interpreting the STM investigation data, it should be remembered that the tunnel current value depends to a greater extent on the density of electron states at $E = E_F$ (E_F is Fermi energy), rather than on the atomic nuclei arrangement. It may well be that here is found the source of differences in the interpretations by different authors of the results of STM investigations. Therefore, we consider theoretical computation and computer simulation an important provision for unambiguous interpretation of STM images of samples in the region of one or the other defect. For HOPG, this was done for the first time in [15] within the framework of strong-bond approximation using the Green function formalism. The results showed that in the case of interstitials (Fig. 3), electron density at the Fermi level changes but insignificantly, because of the large characteristic scale of the lattice deformation (several nm), and there is no interference of the point-defect scattered waves and the normal electron waves. In such situation, the physical mechanism by which the hillocks in the STM images emerge (i.e., the tunnel current increases) is related to the topographic surface change due to lattice stretching by the interstitial atoms. In case of vacancies, there may appear the areas in which the tunnel current also increases (Fig. 4), calling forth their erroneous interpretation as hillocks. Here, current increase is caused solely by electronic interference effects – the growth of electron density at the Fermi level, being confined spatially to the atoms adjacent to vacancies. The actual surface geometry is flat. It was shown that hillocks related to vacancies are smaller in size than those related to interstitials. And finally, it was proved in paper [15] that, for single point defects, the hillocks lateral dimensions differ very insignificantly, and single interpretation in this case is not an easy task. With the growth in the number of point defects

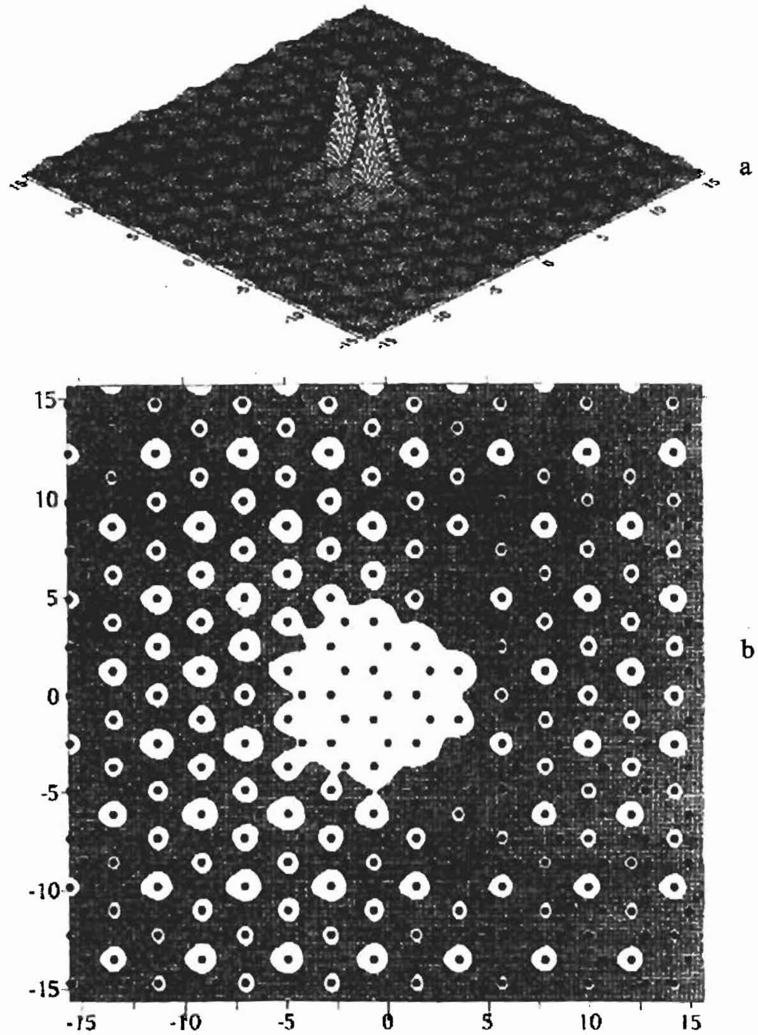

Fig. 3. *Tunnel current density as a function of (x, y) coordinates near a single interstitial atom under the first surface layer of HOPG atoms: a – 3-D picture; b – estimated STM image, 3.0 × 3.0 nm² in size.* U_s *= 0.1 V, h = 0.4 nm. The small dark circles indicate the positions of carbon atoms*

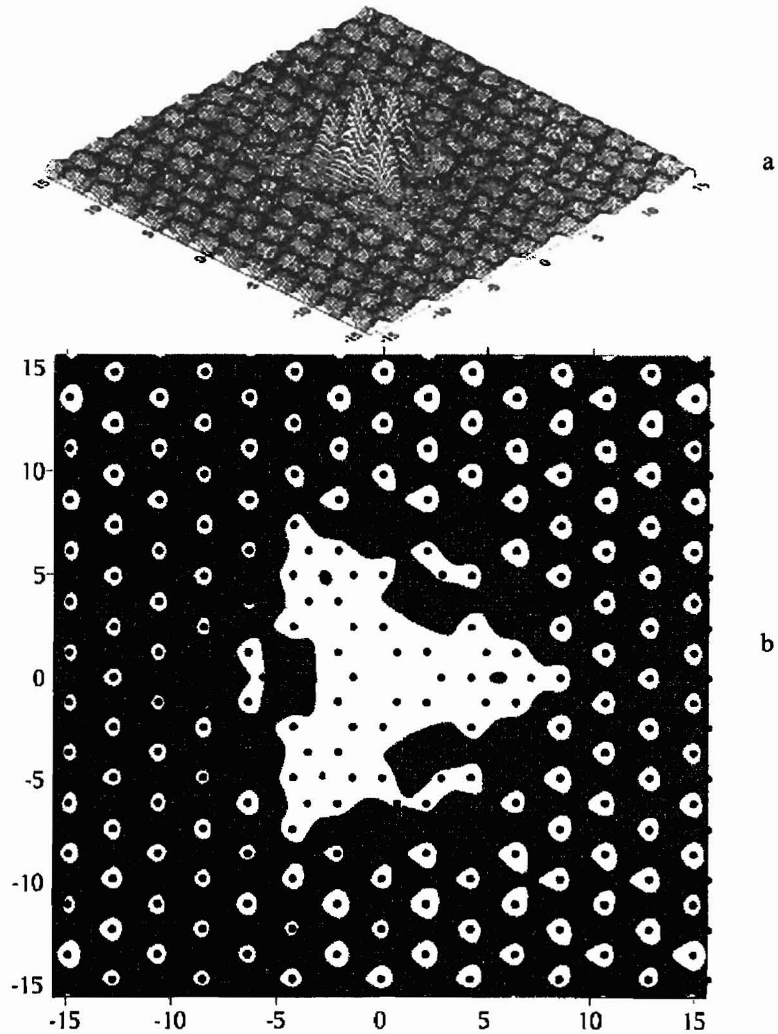

Fig. 4. *Tunnel current density as a function of (x, y) coordinates near a single vacancy in the surface layer of HOPG atoms: a – 3-D picture; b – estimated STM image 3.0 × 3.0 nm² in size.* $U_s = 0.6$ *V,* $h = 0.4$ *nm. The small dark circles indicate positions of carbon atoms.*

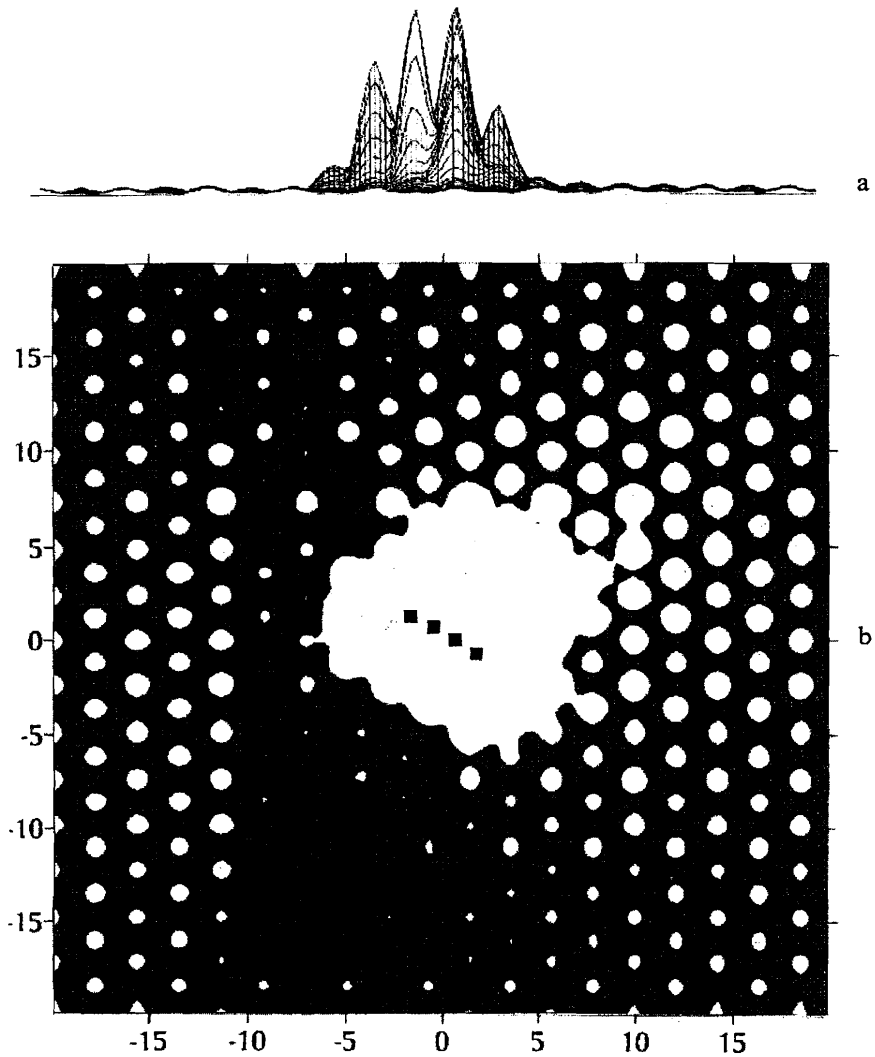

Fig. 5. *Tunnel current density as a function of (x, y) coordinates near a cluster of four interstitial atoms under the first surface layer of HOPG atoms (the interstitial atoms positions are marked with squares): a – 3-D picture; b – estimated STM image 4.0 × 4.0 nm*^{2} *in size.* $U_s = 0.1$ *V,* $h = 0.4$ *nm.*

included in complexes, the sizes of the hillocks formed by interstitial atoms grow linearly with the increase of the complex ratio (Fig. 5), while in the case of vacancies, their change (growth) is insignificant.

VI. EFFECTS OF MATERIALS IRRADIATION WITH LOW-ENERGY PARTICLES

By the present time, there has appeared a big number of publications covering this subject. In the majority of investigations the irradiation fluences were so small that they could ensure appearance of but a few particles in the microscope field of vision, i.e., the traces of single bombarding particles interaction with the sample surface did not overlap. A considerable number of investigations were dedicated to HOPG and silicon. Part of them were carried out in microscopes operating in the air, and a few of them, in SHV-STM, with the participation of the authors of the present paper. Samples of HOPG were irradiated directly in the device with 4.0-keV Ar^+ ions. In all cases, hillocks formation was observed at points of single ion hits (Fig. 6, image size 55.8 × 56.2 nm^2). Their average height reached several tenths of nanometer, with the average base diameter of about 3.0 nm. The surface relief distortion in the region of a single hillock is illustrated in Fig. 7 (field of vision 6.2 × 6.6 nm^2). It would be logical to assume that the observed effect is the result of the development of a cascade of atomic displacements in the sample subsurface region. However, as of today, it appears impossible to derive the cascade parameters from the STM investigation data. Obviously, field ion microscopy [16, 17] may apply as a more reliable method to obtain the data on structure of the defect regions due to single cascades of atomic displacements; at the same time, the authors of the present paper have offered their considerations on the advantages of conducting FIM and STM investigations in parallel [18].

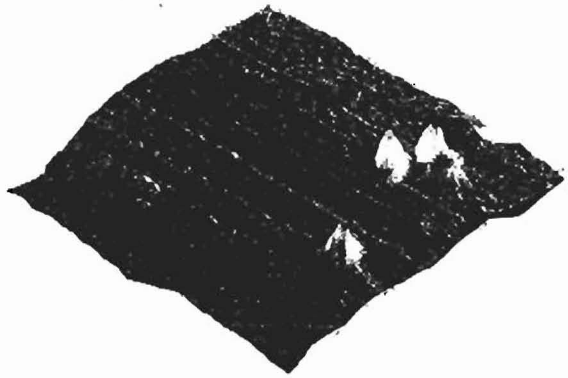

Fig. 6. *Isometric STM image of HOPG sample surface after irradiation with 4.0-keV Ar^+ ions. Picture size: 55.8 × 56.2 nm^2. Each hillock corresponds to a single ion hit.*

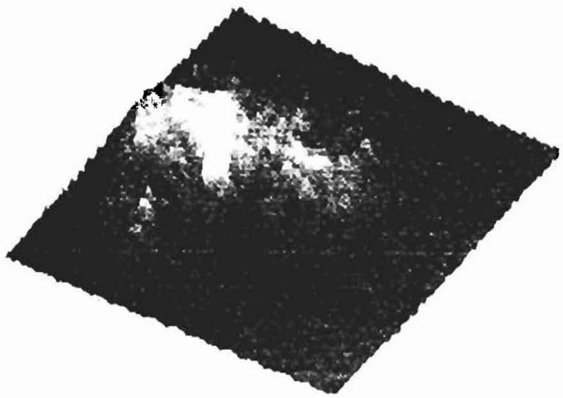

Fig. 7. *Same as in Fig. 6, but with a greater magnification. Picture size: 6.2 × 6.6 nm^2. In the region of the hillock formed by a single ion hit, no atomic-scale resolution has been achieved.*

VII. EFFECTS OF MATERIALS IRRADIATION WITH MEDIUM-ENERGY PARTICLES

An inconsiderable number of presently published papers gives the results of STM analyses of surface profiles of samples irradiated with medium-energy particles. In fact, almost all of the investigations were carried out for the cases of multiple overlapping of the defect regions from single bombarding particles. The authors of the present paper have carried out detailed investigation of the dynamics of change in relief of HOPG surface at its exposure to protons and ions Cs^{+}, Ar^{+}, Xe^{+}, La^{+} irradiation, as well as to SiO_2 high-intensity laser plasma. The ion energies varied from 25 keV to 3.0 MeV. Here, for quantitative evaluation of the degree of surface development, use was made of the notion of fractal dimensions [19]. Based on the experimental values set by the image obtained in STM, profile and surface fractal dimensions were computed by the triangle and pyramid algorithms, respectively. To a considerable degree such analyses were of technical character, being carried out in pursuit of determining the optimal conditions for radiation treatment of HOPG in building flat-shaped field-emission cathodes with a developed surface [20]. An example of one of the STM images of surface of a quite efficient field-emission cathode from HOPG produced by a radiation method is illustrated in Fig. 8. Figure 9 provides the examples to compare the degrees of development of HOPG surfaces after different exposures to irradiation (this is a conventional comparison, since the degree of surface development obtained in practice is determined by a whole complex of such parameters as ion mass and change, ion energy, angle of incidence to surface, particles flux density, irradiation fluence, sample temperature). Some results of the investigations are discussed in [21-23].

The systematic investigations of the effect of proton irradiation on the structure of surface layers in silicon, conducted by the authors, are also oriented to production technology requirements. To a considerable degree they are connected with the development of the processes of manufacture of the so-called silicon-on-insulator structures [24]. As is known, one of the main goals of such structures creation is further miniaturization in electronics. Flat silicon slabs were irradiated with protons with an energy of 700 keV to irradiation fluences varying in the range of 10^{16} to 10^{18} p/cm^2 [25]. In all cases of irradiation, the proton beam was directed square to plane (100). The irradiated samples were then investigated in an STM operating in the air. Prior to STM examination, the sample surface was passivated with tetrafluoroboric acid to recover conductivity. After irradiation, the samples corresponding to fluences above $5 \cdot 10^{17}$ p/cm^2 stood aside from

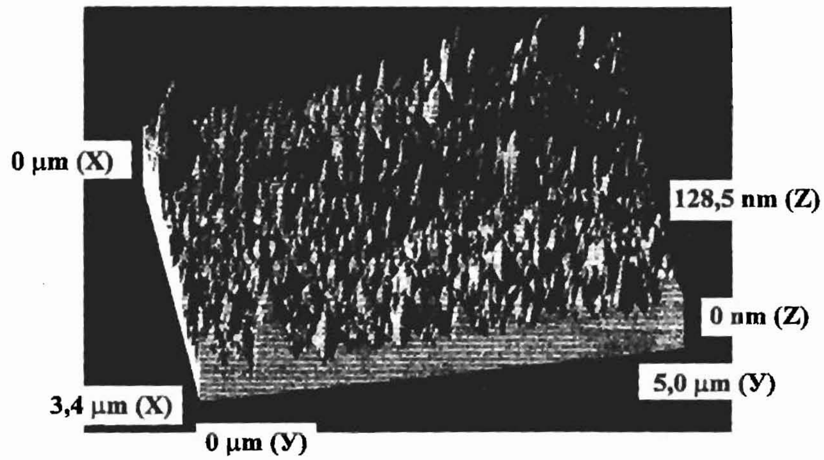

Fig. 8. *Isometric STM image of HOPG sample surface after exposure to SiO_2 high-intensity laser plasma.*

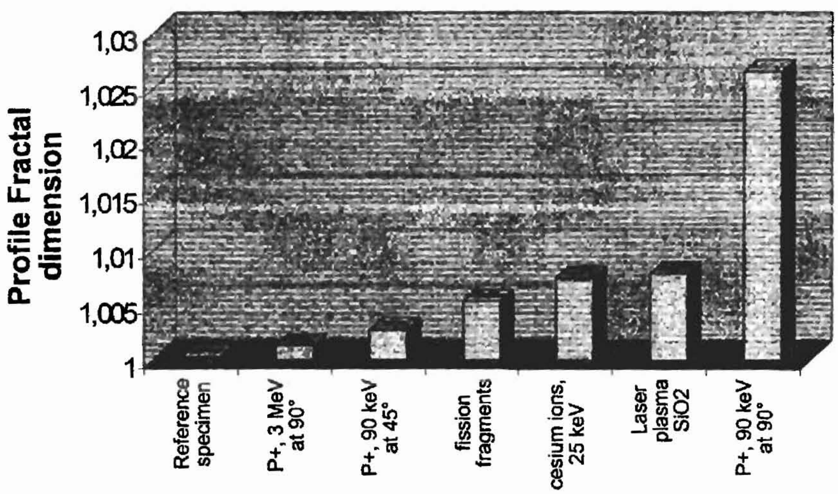

Fig. 9. *Graphic illustration of the degree of HOPG samples surface development after different exposures to irradiation.*

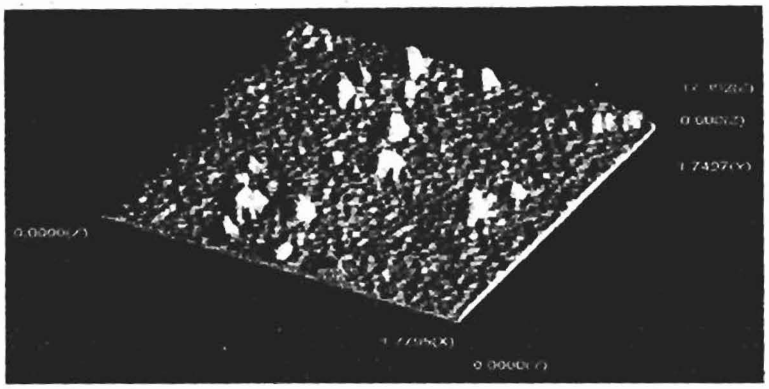

Fig. 10. *Isometric STM image of a silicon sample surface after irradiation with 700-keV protons to fluence of 10^{16} p/cm^2. Picture size: 1.78 × 1.75 μm^2, height-to-height amplitude: 17 nm. Apparently, the hillocks observed on the surface correspond to unbroken blisters.*

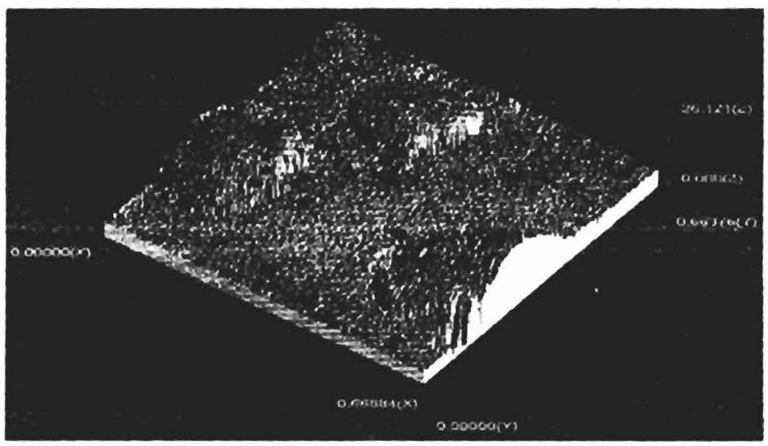

Fig. 11. *Same as in Fig. 10, but with a greater magnification. Picture size: 0.67 × 0.66 μm^2. Three unbroken blisters are observed.*

other samples – not for their better conductivity only, by also for change of their surface visible to a naked eye (temperate colors appeared). The images showed development of single blisters (Fig. 10, 11), which showed a tendency to overlapping with the increase in fluence, and breaking at samples annealing.

VIII. EFFECTS OF MATERIALS IRRADIATION WITH HIGH ENERGY PARTICLES

Only a limited number of publications has appeared so far to cover this direction. The authors of papers [26, 27] observed in the devices operating

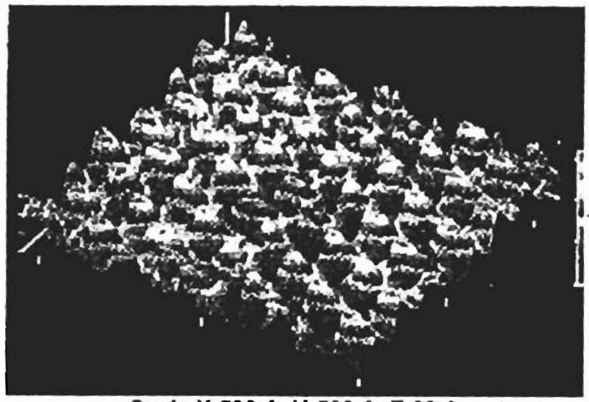

Scale X:500 A Y:500 A Z:20 A

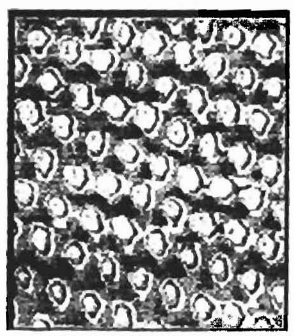

Scale X:500 A Y:500 A Z:20 A

Fig. 12. *Isometric (a) and normal (b) STM image of a HOPG sample after irradiation with 210-MeV Xe^{+} ions. Formation of regularly arranged hillocks is observed.*

in the air the formation of a regular relief on a HOPG surface at its irradiation with 215-MeV Ne^+ ions, and 210 MeV Xe^+ ions, respectively (Fig. 12). It was shown that such kind of a relief is not observed on the entire HOPG surface. Paper [28] offers a theoretical model of such structures formation based on the analysis of distribution by depth of the energy provided by irradiation. The authors see as most promising the use of STM analysis in investigating the effect of preferable sputtering of the surface material in the areas of its imperfections. Most likely, an original information may also be obtained from the STM analyses of single events of interaction of nuclei fission products with surfaces of various materials. The first very encouraging results are provided by the authors in [29].

IX. CONCLUSION

Analysis of the capabilities of scanning tunneling (and atomic-force) microscopy and the presently available results obtained allows us to make the following conclusions.

1. Application of STM and AFM techniques in radiation damage physics of solids and radiation materials science has been found advantageous and promising. New and original results of their application may be anticipated in these fields.
2. "Sub-threshold" radiation effects of point defects formation and quantitative evaluations of crystal lattice deformation in the point defects field are looked upon as an area with the best prospects for STM analysis application. Most practical would be to conduct such investigations in super-high vacuum devices providing an opportunity to implement parallel samples analyses by the methods of Auger- and photoelectron spectroscopy.
3. An important way to unambiguous interpretation of the immediate STM analysis data is development and implementation of the methods of computation and computer simulation of STM images of the sample surfaces containing various defects in the crystal structure.

4. Interesting results may be anticipated from STM analyses of the processes of anomalous sputtering of surface material in the areas of various defects location.
5. The method of STM analysis, including analyses carried out in the devices operating in the air, has prospects for application in radiation technologies refinement (e.g., in designing efficient flat-shaped field-emission cathodes with the developed surface). Here, use of the methods of quantitative evaluation, e.g., fractal dimensions evaluation, is expedient.
6. The task of publishing an analytical review of the results of presently completed STM and AFM investigations of radiation effects in solids, to generalize, classify and compare the respective works has become the task of current concern.

The work was carried out within the scope of Project # 467 financed by the International Science and Technology Center.

REFERENCES

1. G. Binnig, H. Rohrer. // Rev. Mod. Phys., 1987, V.59, P.615.
2. S.S. Magonov, M.-H. Whangbo. Surface Analysis with STM and AFM. Experimental and Theoretical Aspects of Image Analysis. West Sussex, Willey-VCH, 1995.
3. A.V. Eletsky, B.M. Smirnov. // Uspekhi Fizicheskikh Nauk, 1995, V.165, #9, P.977.
4. V.F. Elesin, A.L. Suvorov. Moscow: Preprint ITEP No. 6.
5. Database of ultramicroscopic investigations in the field of radiation physics of solids and radiation materials science (BDUMI-RFFT-BM). Project #467-97 ISTC. Moscow: ITEP, 1999.
6. I.V. Yaminsky, A.L. Suvorov. // Uspekhi Fizicheskikh Nauk, 1999 (in press).
7. V.V. Kirsanov, A.L. Suvorov, Yu.V. Trushin. Protsessy radiatsionnogo obrazovaniya v metallakh. Moscow: Energoatomizdat, 1985.
8. A.M. Parshin et al. Struktura i radiatsionnaya povrezhdayemost konstruktsionnykh materialov. Parts 1 – 3, Moscow: Metallurgiya, 1996.
9. Raspyleniye tverdykh tel ionnoi bombardirovkoi / Edited by R. Berish. Moscow: Mir, 1984 (V.1), 1986 (V.2).
10. B.A. Kalin, D.M. Skorov, V.L. Yakushin. Problemy vabora materialov dlya termoyadernykh reaktorov. Moscow: Energoatomizdat, 1985.
11. G. Schimmel. Metodika elektronnoi mikroskopii. Moscow: Mir, 1972.
12. V.F.Elesin. // Doklady Akademii Nauk, 1988, v.298, p. 1377.
13. R.E. Baranovsky, K.N. Eltsov, V.F. Elesin, A.L. Suvorov, V.M. Shevlyuga, V.Yu. Yurov. // Phys. Low-Dim. Struct., 1999 (in press).
14. K.N. Eltsov, A.N. Klimov, S.L. Priadkin et.al. // Phys. Low-Dim. Struct., 1996, V.7/8, P.115.
15. V.F. Elesin, V.V. Krasheninnikov, L.A. Openov, A.L. Suvorov. Supplement #1 to Technical Report to Project #467-97 ISTC for the 6^{th} quarter, 1999. Moscow: Preprint ITEP No. 25.
16. A.L. Suvorov. Avtoionnaya mikroskopiya radiatsionnykh defektov v metallakh. Moscow: Energoizdat, 1982.

17. A.L. Suvorov. // In coll.: Sovremenniye problemy yadernoi fiziki, fiziki i khimii kondensirovannykh sred. Transactions of the First Moscow International School of Physics of ITEP (Zvenigorod, Moscow Oblast, 17 – 26 February 1998). / Edited by Yu.G. Abov, A.L. Suvorov, V.G. Firsov. Moscow: Editorial Board of Uspekhi Fizicheskikh Nauk Journal, 1999, p. 117.

18. A.L. Suvorov, Yu.N. Cheblukov, N.E. Lazarev, A.F. Bobkov, M.O. Popov, V.P. Babaev. 1998, Moscow: Preprint ITEP No 24.

19. R. Talibuddin, J.P. Runt. // J. Appl. Phys., 1994, V. 76, N 9, P. 5070.

20. I. Brodie, C. Spindt. // Adv. Electron. Electron. Phys., 1992, V. 83, P.1.

21. A.L. Suvorov, E.P. Sheshin, V.V. Protasenko, N.E. Lazarev, A.F. Bobkov, V.P. Babaev. // Zhurnal Tekhnicheskoi Fiziki, 1996, V. 66, #7, P. 156.

22. M.A. Kozodaev, B.A. Loginov, A.L. Suvorov, A.M. Kozodaev. // In coll.: Sovremenniye problemy yadernoi fiziki, fiziki i khimii kondensirovannykh sred. Transactions of the First Moscow International School of Physics of ITEP (Zvenigorod, Moscow Oblast, 17 – 26 February 1998). / Edited by Yu.G. Abov, A.L. Suvorov, V.G. Firsov. Moscow: Editorial Board of Journal: Uspekhi Fizicheskikh Nauk, 1999, P. 241.

23. Yu.N. Cheblukov, A.S. Fedotov, M.A. Kozodaev, B.A. Loginov, M.O. Popov, A.E. Stepanov, A.L. Suvorov, D.N. Volnin. // Materials Science & Engineering A. (in press).

24. V.P .Popov, A.K. Gutakovsky, I.V. Antonova, E.V. Spesivtsev, I.I. Morozov, G.P. Pokhil. // MRS Bulletin 1998, V. 23, #12.

25. M.A. Kozodaev, O.N. Makeev, A.L. Suvorov. // Transactions of the IXth International Conference "Radiation Physics of Solids" (Sebastopol, 28 June – 3 July, 1999), Moscow: NIIPMT, 1999, V.1, P. 352.

26. L.P. Biro, J. Gunlai, K. Havancsak. // Phys. Rev. B., 1995, V. 52, #3, P. 2047.

27. A.L. Suvorov, A.Yu. Didek, Yu.N. Cheblukov, E.P. Sheshin, V.P. Babaev, A.S. Fedotov et. al. // 43rd International Field Emission

Symposium (IFES'96), July 14 –19, 1996, Moscow, Russia. / Program and Abstracts, P. P-90.

28. D.V. Kulikov, A.L. Suvorov, R.A. Suris, Yu.V. Trushin, V.S. Kharlamov. // Pis'ma Zh. Tekh. Fiz, 1997, V. 23, #14, P. 89.

29. M.A. Kozodaev, O.N. Makeev, V.F. Khokhryakov, L.A. Osadchuk, B.G. Levakov, V.P. Babaev, A.L. Suvorov. // Pis'ma Zh. Tekh. Fiz (in press).